

# Tunnel Architectures in Enzyme Systems that Transport Gaseous Substrates

Sukhwinder Singh and Ruchi Anand\*

Cite This: <https://doi.org/10.1021/acsomega.1c05430>

Read Online

ACCESS |



Metrics &amp; More

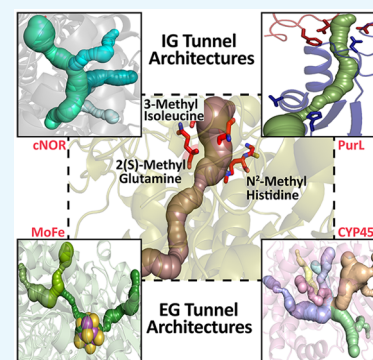


Article Recommendations



Supporting Information

**ABSTRACT:** Molecular tunnels regulate delivery of substrates/intermediates in enzymes which either harbor deep-seated reaction centers or are for transport of reactive/toxic intermediates that need to be specifically delivered. Here, we focus on the importance of structural diversity in tunnel architectures, especially for the gaseous substrate translocation, in rendering differential substrate preferences and directionality. Two major types of tunnels have been discussed, one that transports stable gases from the environment to the active site, namely, external gaseous (EG) tunnels, and the other that transports molecules between active sites, namely, internal gaseous (IG) tunnels. Aspects as to how the gaseous tunnels have shaped during the course of evolution and their potential to modulate the substrate flow and enzymatic function are examined. In conclusion, the review highlights our perspective on the pulsation mechanism that could facilitate unidirectional translocation of the gaseous molecules through buried tunnels.



## INTRODUCTION

Tunnels connect the protein surface to the active site or one active site with the others and serve as conduits for the convenient delivery of molecules. Tunnels transferring small molecules such as  $N_2$ ,  $CH_4$ ,  $C_2H_6$ ,  $O_2$ ,  $CO$ ,  $NH_3$ ,  $H_2$ ,  $C_2H_2$ ,  $NO$ , and  $CO_2$  are termed gaseous tunnels.<sup>1a,b</sup> Conduits that have a surface accessible connection and can accept gases from the surroundings are named external gaseous (EG) tunnels.<sup>2,3</sup> Whereas, buried gaseous tunnels that do not emerge to the surface are named internal gaseous (IG) tunnels.<sup>4,5a,b</sup> In some cases, the tunnels can be preformed, permanently visible within the protein structure such that the natural breathing motions in proteins do not alter the tunnel dimensions to the extent that the radius of the gaseous tunnel falls below the minimum threshold diameter, e.g., carbamoyl phosphate synthetase (CPS) has a preformed tunnel.<sup>6a</sup> In contrast, it can be transient such that the tunnel diameter is not sufficiently wide enough to allow the incoming molecule to pass through it or certain constrictions in the tunnel block its delivery. This could be either to control the frequency of molecules traveling across or to coordinate and facilitate coupled reaction rates.<sup>6b,c</sup> Another possible scenario of transient tunnel formation is one in which the tunnel is nonexistent in the apo state, and only upon significant conformational change, under appropriate cues, is the tunnel formed.<sup>7</sup> In several cases transient tunnels require intermediate/substrate-induced conformational changes in the tunnel residues to open up for the transport of the incoming molecule, within the respective enzyme.<sup>8</sup> These tunnels undergo enormous fluctuations and switch between open and close states, as in formylglycinamide ribonucleotide synthetase (FGAM synthetase) and phosphor-

ibosylpyrophosphate (PRPP) amidotransferase.<sup>8,9</sup> It is remarkable that the presence of these conduits, which are as long as 20–30 Å and even longer like 96 Å in CPS,<sup>6a</sup> run inside the protein body, forming pores that serve as highways for transport of these gaseous molecules. In several cases, an added level of tuning into the tunnel architecture is introduced by incorporating gating mechanisms into the EG and IG tunnel architectures.<sup>6a,10,11</sup>

Gates serve as checkpoints and vary from system to system; some are as simple as an amino acid blocking the path which moves out upon receiving appropriate cues such as the swinging door type in cytidine triphosphate synthase (CTP)<sup>12</sup> and in others more complex arrangement of amino acids come together to form control units such as aperture gates, drawbridge, and shell type gates.<sup>13</sup> These tunnels and their gates are connected via an active communication network that spans between distal centers and hence introduces both conformation and dynamic allostery into the protein systems.<sup>8</sup> It is not uncommon to observe long distance allosteric networks that can be dynamic in nature and transiently formed via the motion of loop elements, secondary structural rearrangements, or of entire domains.<sup>7,8</sup>

In this mini-review, we describe several tunnel architectures and show how they facilitate enzymatic functions. The flow is

Received: September 30, 2021

Accepted: November 22, 2021

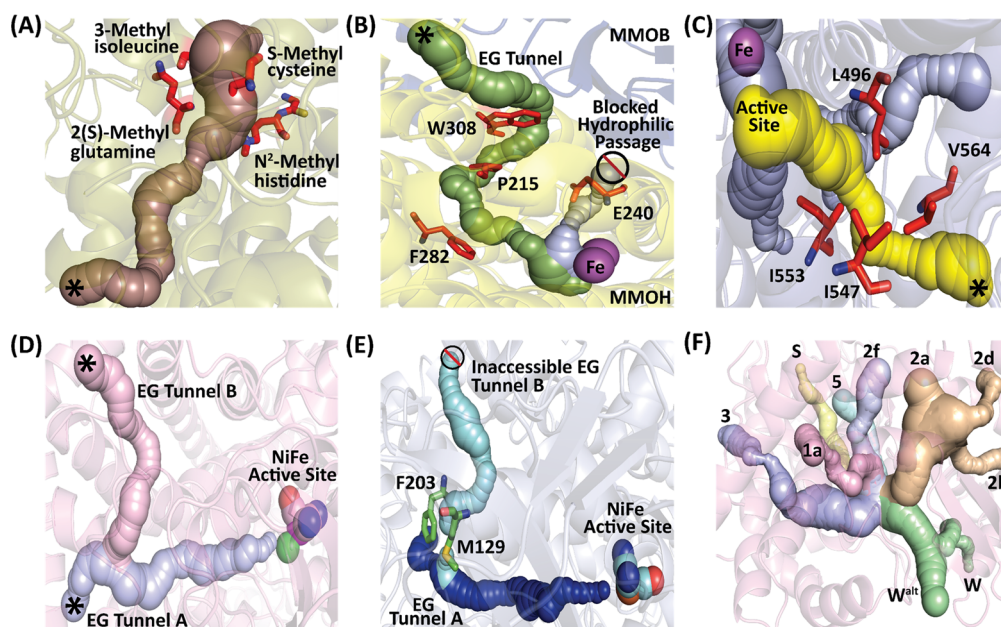


**Figure 1.** EG tunnel architectures: (A) hydrophobic tunnel in ethylCoM reductase harboring post-translationally modified residues near active site end (PDB ID 7B2C, Ni-cofactor  $F_{430}$  not shown). Adapted from ref 14, with permission from AAAS. (B) EG tunnel in MMOH and MMOB complex of *Methylosinus trichosporium* OB3b is shown in green and the blocked hydrophilic passage in light blue color. The gating residues, W308, F282, E240, and P215, are shown as red sticks, and the di-Fe center is shown as magenta spheres (PDB ID 6YDI). Adapted with permission from ref 15a. Copyright 2020 American Chemical Society. (C) The main EG tunnel in soybean lipoxygenase-1 is highlighted in yellow, and the subsidiary tunnels congruent to the view are shown in light blue. Nonheme iron in the active site is shown as a magenta sphere (PDB ID 1YGE). Adapted from ref 2. (D) Two EG tunnels (EG tunnel A in light blue and EG tunnel B in salmon) of *Ralstonia eutropha* NiFe hydrogenase (PDB ID 3RGW). Adapted with permission from ref 3. Copyright 2016 John Wiley and Sons. (E) Inaccessible EG tunnel B and functional EG tunnel A of *E. coli* NiFe hydrogenase are shown in cyan and blue colors. Bulky residues F203 and M129 are depicted as green sticks (PDB ID 3UQY). Adapted with permission from ref 3. Copyright 2016 John Wiley and Sons. (F) Ten EG tunnels of cytochrome P450 monooxygenase, CYP102A1, i.e., 2a, 2b, 2d, 2f, W,  $W^{alt}$ , S, 5, 3 and 1a (PDB ID 2HPD). Adapted with permission from ref 16. Copyright 2016 American Chemical Society. Tunnels identified, in this figure and all the subsequent figures, are drawn using CAVER 3.0 PyMOL plugin.<sup>15b</sup> The asterisk (\*) represents the external end of the tunnel.

divided into discussion of EG and IG tunnels and, in both cases, the unique features and adaptations that the enzymes undertake to perform the requisite function are described. The discussion transitions from architectural preferences and connects the function for enzymes that have a plethora of connected tunnels with the ability of free diffusion to those that have stringent gating requirements for the timely passage of intermediates. Emphasis on directionality and fluctuation in gaseous tunnels that may prevent unnecessary wastage and reflux of the transferred gases is also highlighted.

## EXTERNAL GASEOUS (EG) TUNNEL ARCHITECTURES

EG tunnels connect the bulk solvent with the active site of an enzyme. These tunnels are found in several enzymes that accept gaseous substrates to facilitate their delivery to the buried active site. A class of predominant gaseous substrates are alkanes such as methane and ethane gases that are oxidized aerobically or via anaerobic pathways. Recently, Wagner and co-workers determined the crystal structure of the enzyme that anaerobically oxidizes ethane to ethylCoM from *Candidatus Ethanoperedens thermophilum* and named it ethylCoM reductase (Scheme S1).<sup>14</sup> The enzyme belongs to the broad methylCoM reductase superfamily, which oxidizes methane. It was noted that while none of the methane oxidizing enzymes from this superfamily, such as *Methanothermobacter marburgensis* and the other anaerobic methane-oxidizing archaea, harbor a tunnel (Figure S1), the ethylCoM reductase

counterpart has a 33 Å tunnel that runs across the length of the protein. Interestingly, the EG tunnel present in ethylCoM reductase has some very unique features. At the end of the tunnel, near the Ni-cofactor  $F_{430}$  active site, there are several residues that are post-translationally modified. Methylated amino acids, such as S-methylcysteine, 3-methylisoleucine, 2(S)-methylglutamine, and N<sup>2</sup>-methylhistidine line the tunnel (Figure 1A). It is likely that these residues tune the enzyme to select for ethane by creating a very hydrophobic environment and prevent similar-sized hydrophilic molecules such as methanol from reaching the active center. The larger hydrophobic alkanes are selected out via optimization of the tunnel diameter, which is fit to accommodate ethane.

Another example of an alkane transporting tunnel exists in soluble methane monooxygenase (sMMO) that performs C–H functionalization by breaking the strongest C–H bond, among saturated hydrocarbons, in methane and aerobically oxidizes it to form methanol. In methanotrophs, these enzymes are tightly regulated, and the complex formation between the two proteins, hydroxylase MMOH and regulatory protein MMOB, is required for function. The EG tunnel formed in this system is very hydrophobic, and the diameter is such that it only allows for smaller gases such as methane and O<sub>2</sub> to percolate into the di-Fe cluster harboring active site.<sup>1a</sup> In *Methylosinus trichosporium* OB3b, half of the tunnel is at the interface of the MMOH/MMOB complex, and another half of the tunnel is buried within MMOH, where the oxidation reaction is catalyzed (Figure 1B).<sup>15a</sup> As an added control

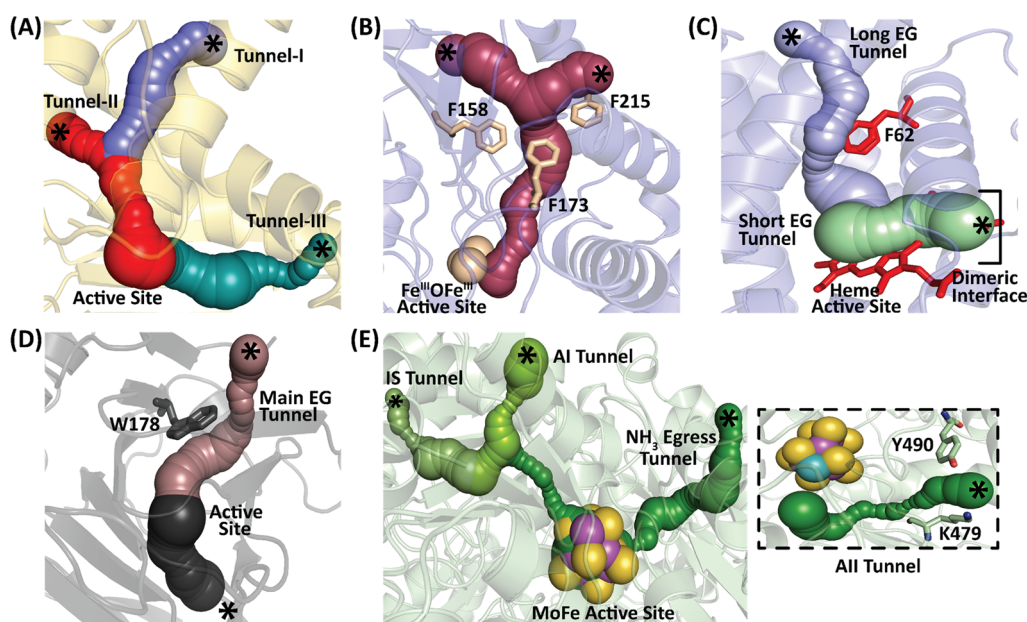


**Figure 2.** EG tunnel architectures: (A) tunnel I (blue), tunnel II (red), and tunnel III (cyan) are shown in H-NOX. The protein structures of *Nostoc sp.* (*Ns*), *Kordia algicida* (*Ka*), and *Caldanaerobacter subterraneus* (*Cs*) are very similar; hence, representative tunnels are drawn on the *Ns* protein structure (PDB IDs 6MX5, 1U55, 6BDD). Adapted from ref 17a. (B) Three phenylalanine residues, F158, F215, and F173, form an  $O_2$  retention zone as depicted in tFprA (PDB IDs 2OHI, 2OHH). Adapted from ref 11 with permission from the Royal Society of Chemistry. (C) A long (gray) and a short (green) EG tunnel in Mt2/2HbN is depicted. The heme group and a gating residue F62 are shown as red sticks (PDB ID SAB8). Adapted with permission from ref 10. Copyright 2015 John Wiley and Sons. (D) Two EG tunnels in AlkB (brown and black) connecting to the active site are shown. The gating residue W178 is shown as gray sticks (PDB ID 2FDG). Adapted from ref 18 with permission from the Royal Society of Chemistry. (E) The four EG tunnels present in nitrogenase: IS, AI, AII, and ammonia egress tunnel (PDB IDs 4WNA, 4WN9). The zoomed view of the AII tunnel is shown in the inset. Adapted with permission from ref 20 (direct link <https://pubs.acs.org/doi/10.1021/bi501313k>). Copyright 2015 American Chemical Society. The asterisk (\*) represents the external end of the tunnel.

feature, the complex has multiple gates to regulate its function. Residues W308 and P215 guard the entrance of the substrate molecules and block the formation of the EG tunnel in the absence of the complex between MMOH and MMOB. Upon complexation, a conformational change is triggered, and these residues move out of the path, opening the passage for the entire tunnel. When the upper gating residues move upon MMOB/MMOH complex formation, another residue F282 right near the active site also concomitantly undergoes a shift, allowing methane and oxygen to access the di-Fe center. MMOH also has an alternative secondary hydrophilic passage, accessible only when MMOB/MMOH complex dissociates which allows the polar methanol product to be released through it. The gating residues, F282 in the hydrophobic EG tunnel and E240 in the hydrophilic passage, switch between open and close states alternately upon binding/unbinding of MMOB and hence opens one of the two tunnels at a time. This regulates the flow of substrates and products and avoids overoxidation of methanol by releasing it through the hydrophilic passage prior to the entry of substrates in the active site via the hydrophobic EG tunnel.

One of the most common gaseous substrates for which several examples of tunneling enzymes exist is  $O_2$ .<sup>2,3,16</sup> It is used in several important oxidation reactions for the generation of essential pathway intermediates and also is a key transport gas in cells. Interestingly in several cases, oxygen is transported to the desired site via molecular tunnels, perhaps to modulate its flow. There are two types of tunnel architectures that are prevalent and have evolutionarily evolved: first, where there is a main tunnel connected to several subsidiary tunnels, and second, those with fewer

tunnels but with stringent gating controls.<sup>10,11,16</sup> For instance, soybean lipoxygenase-1 is an example of a multitunnel system that has eight EG tunnels, out of which the one that is formed by hydrophobic residues, such as L496, I553, I547, and V564, has the highest throughput and is identified as the main gaseous tunnel for delivering  $O_2$  to the reaction center (Figure 1C).<sup>2</sup> It catalyzes the stereospecific peroxidation of linoleic acid via forming a pentadienyl radical intermediate (Scheme S2). Under oxygen-deficient conditions, the intermediate escapes from the active site to the bulk and forms four products, i.e., 13S-, 13R-, 9S-, and 9R-hydroperoxy-octadecadienoic acid, in equal distributions.<sup>2</sup> However, under ambient  $O_2$  conditions, the EG tunnel delivers  $O_2$  efficiently into the active site which has a properly positioned and oriented radical intermediate. Here,  $O_2$  is delivered by the EG tunnel such that it stereo- and regiospecifically attacks (Figure S2) the radical intermediate to yield 13S-hydroperoxy-octadecadienoic acid as a major product with ~90% yield.<sup>2</sup> It has also been shown that when the EG tunnel residue L496 is mutated to a bulky tryptophan, it opens up a new gaseous tunnel for  $O_2$  delivery, where it attacks at the different side of the pentadienyl intermediate, preferring the formation of 9S- and 9R-products.<sup>2</sup> This example showed the importance of the gaseous tunnel in determining the stereo- and regiospecificity for product formation.

Another example of a multitunnel system includes NiFe hydrogenases that catalyze the reversible heterolytic dissociation of  $H_2$  generating  $H_2O$ . These enzymes are divided into two classes,  $O_2$  sensitive and  $O_2$  tolerant.<sup>3</sup> A greater number of accessible gaseous tunnels in these NiFe hydrogenases leads to  $O_2$  sensitivity in these enzymes, and shutting down the

accessibility in some of the EG tunnels renders O<sub>2</sub> tolerance. For instance, in *Desulfovibrio vulgaris* NiFe hydrogenase, there is a network of tunnels that connect the NiFe reaction center to the external environment that allows multiple access routes for O<sub>2</sub>, rendering this system O<sub>2</sub> sensitive.<sup>3</sup> Whereas O<sub>2</sub> tolerant membrane-bound NiFe hydrogenase from *Ralstonia eutropha* harbors only two hydrophobic EG tunnels, tunnel A and tunnel B (Figure 1D).<sup>3</sup> The two tunnels with different entrances merge before extending to the NiFe active site. In *E. coli*, the junction point of these EG tunnels A and B has bulky gating residues F203 and M129, which permanently shut tunnel B, while the EG tunnel A remains operative (Figure 1E). This variation in tunnel accessibility changes the profile of the enzyme from the less O<sub>2</sub> tolerant to a more tolerant system in *E. coli*, which essentially means that the *E. coli* enzyme is more robust and can withstand higher external O<sub>2</sub> concentrations. Regulation of O<sub>2</sub> in these systems is important as excess O<sub>2</sub> leads to oxidation of the NiFe metal center leading to enzyme inactivation.

Cytochrome P450 monooxygenase, CYP102A1, from *Bacillus megaterium* also possesses a tunnel network comprising several shared tunnels for delivering substrates of diverse types, i.e., gaseous substrate O<sub>2</sub>, and an organic substrate, fatty acid.<sup>16</sup> A large number of access points to O<sub>2</sub> likely are a result of the importance of maintaining the integrity of this reaction as metabolism of the fatty acid variants, steroids, and synthesis of hormones are crucial and essential for cell survival. For O<sub>2</sub> delivery from bulk to the active site, ten EG tunnels have been identified in CYP102A1, which are the 2a, 2b, 2d, 2f, W, W<sup>mt</sup>, S, S, 3, and 1a tunnels (Figure 1F).<sup>16</sup> The EG tunnels 2a, 2b, 2d, and 2f transfer not only the gaseous substrate O<sub>2</sub> but also the fatty acid substrates. The tunnel S, a short tunnel with a small diameter, possesses the least activation barrier for the O<sub>2</sub> delivery and is accessible to the solvent molecules as well. Tunnel W offers the highest activation barrier and is the least preferred EG tunnel for O<sub>2</sub> delivery to the active site.<sup>16</sup> Another remarkable feature of this tunnel design is that a tunnel-to-tunnel O<sub>2</sub> transfer takes place between the two EG tunnels 2b and 2f. This unusual transfer has been proposed to occur via transiently formed bridges between these tunnels.<sup>16</sup>

Another example where O<sub>2</sub> tunnels exist is in nitric oxide and oxygen-binding domain (H-NOX) proteins, which are heme-based sensing proteins known to deliver O<sub>2</sub> in the tumor cells under hypoxic conditions.<sup>17a</sup> Ligand coordination is strengthened here by back bonding between metal d orbitals and ligand  $\pi^*$  antibonding molecular orbitals. The EG tunnel network in H-NOX has been studied in three bacterial species, i.e., *Nostoc sp.* (*Ns*), *Kordia algicida* (*Ka*), and *Caldanaerobacter subterraneus* (*Cs*). Three EG tunnels have been identified in H-NOX (Figure 2A) and, out of which, at least two tunnels are preferred for the substrate translocation in *Ns* H-NOX, *Ka* H-NOX, and *Cs* H-NOX. Out of three EG tunnels, one is a long hydrophobic tunnel (tunnel-I), while the other two are short and slightly polar (tunnel-II and tunnel-III).<sup>17a</sup> Tunnel-I is accessible and is utilized for substrate translocation in both *Ns* H-NOX and *Ka* H-NOX, making the escape of O<sub>2</sub> very facile through it. A unique aspect of this O<sub>2</sub> transport in this system is that the tunnel provides a funneling effect which helps regulate O<sub>2</sub> release and additionally provides specificity to the transport process when compared with other heme systems like myoglobin which also act as oxygen carriers.

An upgrade into O<sub>2</sub> tunneling enzymes are systems that possess fewer O<sub>2</sub> tunnels but stringent gating controls.

Flavodiiron protein *tFprA*, an oxidase found in *Methanothermococcus thermolithotrophicus*, is one such example.<sup>11</sup> The Fe-containing enzyme converts O<sub>2</sub> into two molecules of H<sub>2</sub>O by using flavin mononucleotide (FMN) and the reduced form of deazaflavin derivative F<sub>420</sub>H<sub>2</sub> as cosubstrates.<sup>11</sup> An EG tunnel with two entrances helps in transferring O<sub>2</sub> from bulk to the active site (Figure 2B). The bifurcated EG tunnel in *tFprA* merges to a region containing three phenylalanine residues that are responsible for regulating the O<sub>2</sub> flow. This creates a high O<sub>2</sub> affinity region at the junction point of the tunnels forming an oxygen-retention zone in the middle of the EG tunnel, which decreases the O<sub>2</sub> flow toward the active site of *tFprA*, thereby preventing inactivation of the enzyme.<sup>11</sup>

Other examples of the enzyme with complex control for delivery of O<sub>2</sub> are in the oxygen-sensing regime.<sup>17b</sup> For instance, the hypoxia inducible factor-1 (HIF-1) and prolyl hydroxylase domain enzyme 2 (PHD2) play an essential role by participating in an oxygen-sensing system that senses hypoxia in animals.<sup>17b</sup> HIF-1 comprises two separate subunits, HIF- $\alpha$  and HIF- $\beta$ ; here, the hydroxylation of P402 and P564 in HIF- $\alpha$  by PHD2, using  $\alpha$ -ketoglutarate, and O<sub>2</sub>, under normal O<sub>2</sub> conditions, prevents HIF- $\alpha$  to form a complex with HIF- $\beta$ .<sup>17b</sup> Though PHD2 performs hydroxylation of HIF- $\alpha$  using O<sub>2</sub> under normal conditions, the rate of this reaction is very slow. This is attributed to the presence of the hydrophobic EG tunnel that has a narrow entrance, which slows down the transport of O<sub>2</sub> to the active site present in PHD2. In this case residues from both PHD2 and HIF- $\alpha$  participate to form a functional EG tunnel. The lower reaction rate in this enzymatic system tuned by the presence of the hydrophobic tunnel is a desirable property to create an efficient O<sub>2</sub> sensing system, highly sensitive to the hypoxic environment. This example shows that gaseous tunnels do not always ease the substrate transportation, rather both in the HIF- $\alpha$ /PHD2 system and *tFprA*, the tunnels impose a fine control on reactivity by slowing down the substrate diffusion.

To keep the accessibility of molecular tunnels intact for the gaseous substrates, the structural aspect of the protein also plays a significant role, as is the case of *Mt2/2HbN*, found in *Mycobacterium tuberculosis*. This enzyme is evolutionarily distinct and possesses a unique structural feature that is not found in other truncated hemoglobins. It possesses an oxygen-dependent NO dioxygenase activity for relieving nitrosative stress.<sup>10</sup> *Mt2/2HbN* has two hydrophobic EG tunnels that are nearly orthogonal to each other, a long EG tunnel and a short EG tunnel (Figure 2C).<sup>10</sup> In deoxygenated form, phenylalanine (F62), a gating residue in the long EG tunnel, attains a conformation where the tunnel is closed and partially blocks O<sub>2</sub> delivery. Therefore, O<sub>2</sub> is proposed to be transferred via the short EG tunnel. Once O<sub>2</sub> binds with heme, it induces conformational changes that allow NO to enter through the long EG tunnel. *Mt2/2HbN* has another unique feature, it harbors a N-terminally located pre-A region whose truncation promotes dimerization.<sup>10</sup> As a result of truncation in *Mt2/2HbN*- $\Delta$ preA, the accessibility to the gaseous substrates is lost via the short tunnel as it extends from the active site to the dimeric interface, and thus, it is completely blocked. The dimerization also restricts the F62 in a closed conformation, thereby tuning access to NO via the long EG tunnel and results in the reduction of NO dioxygenase activity by 35-fold in *Mt2/2HbN*- $\Delta$ preA.<sup>10</sup>

Apart from complexation, gating, and multiple passages, another route adopted by enzymes to control O<sub>2</sub> delivery is to

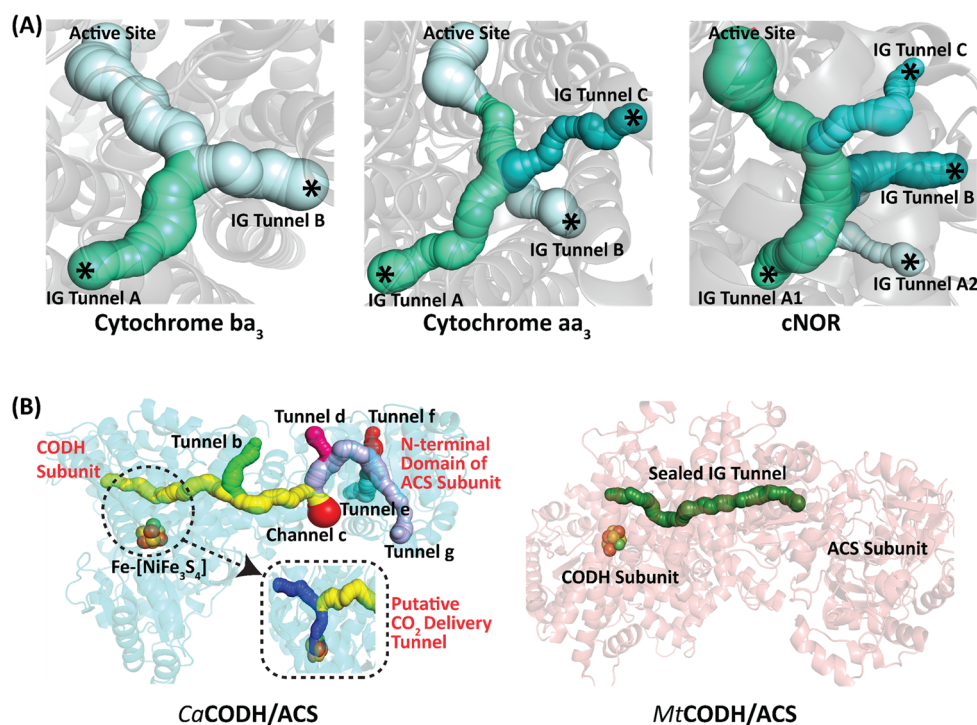


**Figure 3.** IG tunnel architectures: (A) IG tunnels in Cytochrome  $ba_3$ , Cytochrome  $aa_3$ , and Cytochrome c dependent nitric oxide reductases cNOR (PDB IDs 1XME, 1A81, 5GUX). Adapted from ref 5a, Copyright 2018, with permission from Elsevier. The asterisk (\*) represents the tunnel entry point(s). (B) Porous IG tunnel in CaCODH/ACS and sealed IG tunnel in MtCODH/ACS. CaCODH/ACS has seven EG tunnels connected to the IG tunnel; a putative CO<sub>2</sub> delivery tunnel (blue), tunnel b (green), channel c (red), tunnel d (pink), tunnel e (cyan), tunnel f (red), and tunnel g (gray) (PDB ID 6YTT). MtCODH/ACS has a sealed IG tunnel (dark green) (PDB ID 1MJG). Adapted from ref 4, Copyright 2021, with permission from Elsevier.

introduce fluctuations in the tunnel. Enzymes such as *E. coli* AlkB, which performs an oxidative dealkylation of the alkylated bases in the damaged DNA, adopt this approach.<sup>18</sup> Two EG tunnels have been identified for delivering O<sub>2</sub> to the reaction center, with one of the EG tunnels having a lesser curvature than the other. This tunnel also harbors a gating residue W178 for regulating the flow of O<sub>2</sub> through it and is the main EG tunnel in AlkB (Figure 2D). The fluctuating nature of this gaseous tunnel affects the time spent by the O<sub>2</sub> molecule in the active site, thereby controlling its reactivity. The fluctuations in the tunnel could be altered by mutating the tunnel residues.<sup>18</sup> For instance, by mutating the gating residue, tryptophan, to tyrosine, the fluctuations in the tunnel became diminished, and as a result, O<sub>2</sub> spends more time in the active site of AlkB.<sup>18</sup> Thus, dynamics within the gaseous tunnel help hold the substrate in the active site and affects the enzyme activity.

Besides O<sub>2</sub>, there are enzymes that tunnel other stable gas molecules, such as CO<sub>2</sub> and N<sub>2</sub>. For instance, a class of carbonic anhydrase (CA) enzymes, namely, zeta ( $\zeta$ ) CA, catalyzes the hydration of CO<sub>2</sub> to HCO<sub>3</sub><sup>-</sup> and H<sup>+</sup>, harboring a CO<sub>2</sub> tunnel.<sup>19</sup> Such a tunnel has not been observed in the other studied members of the CA family ( $\alpha$  and  $\beta$  CA).<sup>19</sup> Recent structural and theoretical studies performed on  $\zeta$  CA have revealed an L-shaped hydrophobic EG tunnel that additionally allows these enzymes to accept a more hydrophobic substrate, CS<sub>2</sub>.<sup>19</sup> Thus enabling  $\zeta$  CA to catalyze the conversion of CS<sub>2</sub> into H<sub>2</sub>S.

Nitrogenase catalyzes the conversion of highly inert and stable gaseous molecular N<sub>2</sub> into NH<sub>3</sub> by consuming six protons and six electrons.<sup>20</sup> This enzyme houses an unusual homocitrate bonded molybdenum–iron (MoFe) cluster in its

active site that has adequate reducing potential to carry other reactions such as reduction of two H<sup>+</sup> ions into H<sub>2</sub> and can reduce nonphysiological gaseous substrates such as acetylene and propyne.<sup>20</sup> For the transport of nonpolar gaseous molecules, such as N<sub>2</sub>, H<sub>2</sub>, etc., three EG tunnels have been identified, namely, AI, AII, and IS tunnels (Figure 2E).<sup>20</sup> The two predominantly hydrophobic EG tunnels, AI and IS, originate from different regions of the protein surface but fuse in the middle giving a Y-shaped architecture. Since N<sub>2</sub> reduction generates two polar NH<sub>3</sub> molecules, to avoid interference, a separate EG tunnel called the ammonia egress tunnel,<sup>20</sup> which is primarily hydrophilic, facilitates the release of ammonia to the bulk. This system showcases a fascinating tunnel architecture having separate hydrophobic and hydrophilic conduits for polar and nonpolar gaseous moieties.

As the last example of an EG tunnel, we discuss a case where O<sub>2</sub> is a product of the reaction. A unique gaseous tunnel network has been found in Photosystem II (PSII). PSII catalyzes the conversion of water into O<sub>2</sub> along with the reduction of plastoquinone using solar energy.<sup>21</sup> It has three EG tunnels for ejecting the O<sub>2</sub> molecule into the lumen and five water channels for transferring H<sub>2</sub>O to the active site containing the Mn<sub>4</sub>CaO<sub>5</sub> cluster.<sup>21</sup> These EG tunnels, for O<sub>2</sub> transfer, are not hydrophobic but significantly overlap with the water-conducting channels. H<sub>2</sub>O and O<sub>2</sub>, which have entirely different polarities and different sizes, share the common tunnel network but are transferred in the opposite direction. The permeability of the tunnels is different for these two molecules. The rate of O<sub>2</sub> permeation through these tunnels is 1100 times faster than the H<sub>2</sub>O permeation rate as these tunnels offer a lower activation barrier to O<sub>2</sub>.<sup>21</sup> Thus, the

tunnel framework is such that it helps in ejecting O<sub>2</sub> from the active site very quickly and avoid the formation of reactive oxygen species that are detrimental to the function of PSII.

## INTERNAL GASEOUS (IG) TUNNEL ARCHITECTURES

While the EG tunnels transport gases and have pores that are accessible to the surface, there is another class of tunnels formed within the core of the enzyme system, buried in the body of the protein, called the IG tunnels. The need for IG tunnels arose to efficiently translocate reactive gaseous molecules that can either be toxic to the cell or are reactive intermediates that need to be delivered to complete a coupled reaction. These systems generally have the tunnel connecting two reactive centers, and the product of one reaction is transported to the second active site. In some cases, an IG tunnel network, instead of leading to another active site, can also lead to the lipid membrane so as to directly access the active site of membrane-bound enzymes.<sup>5a</sup> An example of such systems where enzymes embedded in the lipid bilayer have gaseous tunnels facing the lipid membrane are the O<sub>2</sub> and NO transporting class of cytochrome b<sub>3</sub>, cytochrome aa<sub>3</sub>, and cytochrome c dependent nitric oxide reductase cNOR.<sup>5a</sup> These enzymes belong to the heme-copper oxidoreductase superfamily, containing multiple heme centers. While cytochrome b<sub>3</sub> and cytochrome aa<sub>3</sub> catalyze the reduction of O<sub>2</sub> to H<sub>2</sub>O, cNOR catalyzes the conversion of NO to nitrous oxide.<sup>5a</sup> These enzymes have hydrophobic tunnels and absorb NO and O<sub>2</sub> from the lipid membrane. Cytochrome b<sub>3</sub> has two IG tunnels, A and B, which merge to form a single tunnel that leads to the active site, whereas cytochrome aa<sub>3</sub> has an additional IG tunnel C along with A and B (Figure 3A).<sup>5a</sup> However, in each system, the diameter of these tunnels varies, i.e., in cytochrome b<sub>3</sub>, tunnels are larger in diameter as opposed to the narrow tunnels in cytochrome aa<sub>3</sub>, which has constrictions. Consequently, O<sub>2</sub> transport is 10 times slower in the latter enzyme. Similarly, cNOR, which has four IG tunnel entrances (IG tunnel A1, A2, B, and C), has two bottlenecks in NO transferring tunnels and results in a 3-fold decrease in the rate of substrate delivery as compared to cytochrome b<sub>3</sub>.<sup>5a</sup>

Another class of IG tunnels are those that are involved in the transport of reactive gases such as CO and NH<sub>3</sub>. Since CO can be toxic to the surrounding environment and may get oxidized to CO<sub>2</sub> under aerobic conditions, coupled active site systems that generate CO and later use it as a substrate for the subsequent reaction have IG tunnels. There are multiple types of CO transporting systems with different architectural preferences, which impresses the impact of evolution on gaseous tunnels. For instance, the IG tunnel in carbon monoxide dehydrogenase/acetyl CoA synthase (CODH/ACS) enzyme isolated from two species, namely, *Moorella thermoacetica* and *Clostridium autoethanogenum*, harbor varied tunnel architectures.<sup>4</sup> CODH/ACS is a multisubunit bifunctional enzyme where the CO<sub>2</sub> is converted to CO at the first active site having a Fe-[NiFe<sub>3</sub>S<sub>4</sub>] cluster which is then transported to the second active site via a 70 Å long IG tunnel.<sup>4</sup> At this receiver active site, CO is incorporated into HSCoA via another Fe-S-Ni cluster which utilizes three different sized substrates, i.e., HSCoA, CO, and methyl bonded corrinoid FeS protein, thereby catalyzing the synthesis of acetyl CoA. The IG tunnels for transporting CO in *Ca*CODH/ACS and *Mt*CODH/ACS are quite different. The former has an IG tunnel with many accessory EG tunnels linked to a long central

tunnel, while the latter has a totally sealed IG tunnel (Figure 3B). There is a total of seven EG tunnels in *Ca*CODH/ACS, out of which two are hydrophobic.<sup>4</sup> One of these hydrophobic EG tunnels is hypothesized to be a putative CO<sub>2</sub> delivery tunnel, which facilitates CO<sub>2</sub> transport between bulk and CODH active site. The porous nature of the IG tunnel in *Ca*CODH/ACS is advantageous during high CO concentration in the system, and it is envisioned that the accessory EG tunnels provide bidirectionality to CO in *Ca*CODH/ACS. On the contrary, the lack of accessory EG tunnels in *Mt*CODH/ACS seems to point toward a unidirectional transport system and is likely a thermophilic adaptation aimed to limit diffusion of CO at elevated temperatures by providing a compact architecture. Moreover, it was noticed that the putative CO<sub>2</sub> delivery tunnel in *Ca*CODH/ACS is a preformed one. However, the tunnel in *Mt*CODH/ACS for CO<sub>2</sub> delivery is dynamic in nature as it could not be trapped in its static X-ray crystal structure.<sup>22</sup> MD simulations on the *Mt*CODH/ACS also reveal that during the oxidative addition reaction of CO<sub>2</sub> itself, an intermediate state is formed where a hydroxyl group is ligated to the metal center in CODH active site and gets involved in the formation of a strong H-bonding network toward the dynamic CO<sub>2</sub> delivery tunnel side, thereby occluding this path for CO to escape after release.<sup>22</sup> This directs the CO solely toward the ACS active site via the long hydrophobic IG tunnel providing directionality.

The next class of gaseous tunnels, which are ubiquitous in nature and exist with several architectural preferences, are the NH<sub>3</sub> transporting tunnels. These tunnels are either preformed as in an example of CPS discussed subsequently or can be transient. In most cases, an IG tunnel is necessary as NH<sub>3</sub> released in the coupled reaction system acts as a nucleophile in the second reaction, and therefore, it has to be protected from the solvent to prevent the formation of NH<sub>4</sub><sup>+</sup> ion. Glutamine amidotransferases (GATases) are the enzymes that synthesize ammonia via the conversion of glutamine to glutamate.<sup>1b</sup> They have two primary classes: while Class II has a N-terminal cysteine residue which facilitates the reaction, Class I harbors a cysteine, histidine, and aspartic/glutamic acid catalytic triad that catalyzes the formation of ammonia.<sup>1b,23</sup> To facilitate ammonia transfer, two broad strategies are exploited by nature. In the first, the GATase is a separate enzyme, and only upon complexation with the receiver domain, it gets activated and, subsequently, NH<sub>3</sub> is channeled. In the second, the GATase and receiver domain exist as subunits within the larger polypeptide, and activation of the amidotransferase unit occurs when substrates are present in both the active sites. Concomitantly in these cases, the NH<sub>3</sub> tunnel is formed via appropriate conformation changes. The de novo purine biosynthetic pathway responsible for the synthesis of purine bases, which serve as precursors to DNA and RNA, is an example where several NH<sub>3</sub> tunneling enzymes exist. For instance, the first step of the pathway is catalyzed by PRPP amidotransferase, a class II enzyme that catalyzes the conversion of PRPP to phosphoribosylamine. Smith and co-workers demonstrated that in the presence of diazo-5-oxonorleucine and a carbocyclic analogue of PRPP, ~20 Å hydrophobic tunnel is formed that connects the amidotransferase domain with the PRPP active site.<sup>9</sup> Several structural elements, including bending of the helix that caps the PRPP moiety, and conformational changes such as the ordering of flexible loop formed by Val 325 to Arg 354 as well as the

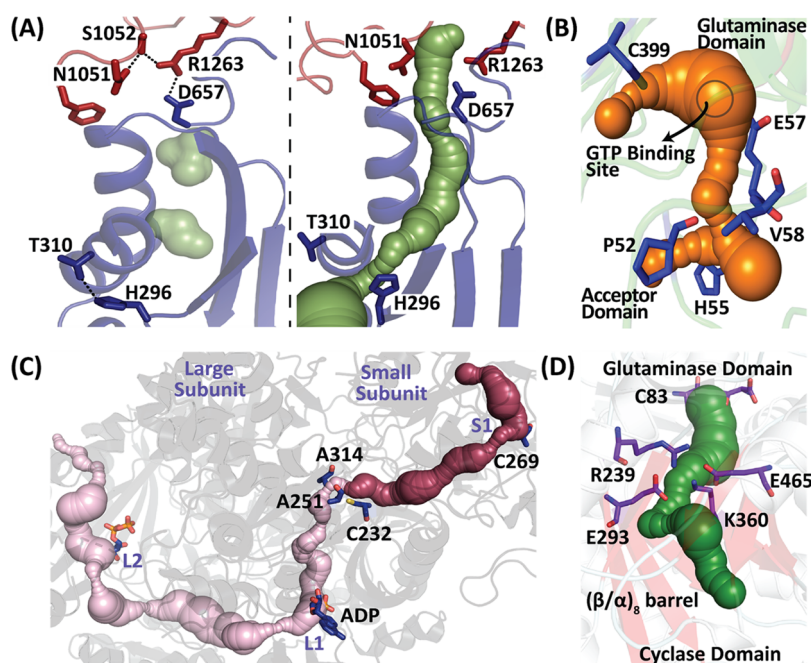


**Figure 4.** Different ammonia tunnels: (A) hydrophobic transient ammonia tunnel in FGAM synthetase has a mouth gate formed by residues S1052, N1051, R1263, and D657 and an end gate formed by T310 and H296 (PDB ID 1T3T).  $\text{NH}_3$  tunnel is transient in FGAM synthetase, and only upon appropriate conformational changes originating at the end gate, it becomes accessible. (B)  $\text{NH}_3$  tunnel in *dmCTP* Synthetase has a GTP binding site. The tunnel lining residues are represented as blue sticks (PDB IDs 6L6Z, 6LFG, 7DPT, 7DPW). Adapted from ref 12. (C)  $\text{NH}_3$  tunnel in CPS originates from the S1 active site and ends at the L1 active site via a triangular gate A314-A251-C232 (PDB ID 1C3O). Adapted with permission from ref 6a. Copyright 2009 American Chemical Society. (D) The IGPS ammonia tunnel (green) passes through the  $(\beta/\alpha)_8$  barrel. The charged gating residues in the middle of the tunnel are shown in purple (PDB ID 1JVN). Adapted from ref 24, Copyright 2001, with permission from Elsevier.

reorientation of loop region formed by Arg 73 to Ser 79 participate in completing the tunnel.<sup>9</sup>

Another example of the transient  $\text{NH}_3$  tunnel system is the fourth enzyme in the purine biosynthetic pathway, FGAM synthetase. This enzyme exists in two forms. In eubacteria and eukaryotes, it is a large protein of over 1200 amino acids having a single polypeptide chain that harbors both the GATase and FGAM synthetase catalytic domains, namely, IgPurL.<sup>6b</sup> In archaea and Gram-positive species such as *Bacillus subtilis*, three different proteins, i.e., a GATase, FGAM synthetase, and an adaptor protein, come together in the presence of ADP to form a functional complex.<sup>8</sup>  $\text{NH}_3$  that is produced in the GATase domain, named G-site, is channeled via a transient tunnel,  $\sim 25$  Å long, to the FGAM synthetase domain, named the F-site. Like PRPP, it has been shown by Anand and co-workers by studying *Salmonella typhimurium* IgPurL as a model system that only when substrates are present in both the G- and the F-sites is the tunnel fully formed.<sup>8</sup> A striking feature of this enzyme is the presence of two gates, one formed at the mouth of the tunnel near the GATase site, comprising of residues R1263, D657, N1051, and S1052 and another at the base (end-gate), consisting of H296 and T310 near the F-site.<sup>8</sup> The mouth gate operates by forming a dynamic hydrogen bonding network and controls  $\text{NH}_3$  transport (Figure 4A).<sup>8</sup> The end-gate seems to play a dual role and signals the entry of the substrate formylglycinamide ribonucleotide (FGAR) and ATP to the rest of the protein and also participates in the formation of the iminophosphate intermediate.<sup>8,6b</sup> Moreover, it initiates a complex and intricate relay of allosteric communication that originates at the synthetase site and transports the signal via the N-terminal adaptor domain to the G-site. The transient tunnel formed is

mostly hydrophobic, and it has been established via MD simulation that during the course of the reaction, the tunnel fluctuates between open and closed phases somewhat like a breathing motion (unpublished results). Whether this helps in reducing wasteful ammonia leakage or it is to provide directionality to the process is unclear and needs to be further explored.

Guanosine 5'-monophosphate synthetase (GMPS) is another enzyme that harbors a transient tunnel. In this enzyme, ammonia is transferred from the GATase domain to the ATP pyrophosphatase domain, which converts an ATP activated xanthine monophosphate to guanosine monophosphate.<sup>7</sup> It has been proposed in the *Plasmodium falciparum* version of the enzyme by Balaram and co-workers that the formation of the transient  $\text{NH}_3$  tunnel in GMPS is driven by the  $85^\circ$  rotation of the entire GATase domain, which purports the conformational changes in a helix stretch, spanning residues 371–395, and another 25 amino acid long loop linked to this helix, which seals the external environment creating the ammonia tunnel.<sup>7</sup>

A differential way of modulating transient tunnel formation that showcases the vast architectural diversity in the  $\text{NH}_3$  tunnel design is in CTP synthase. The *Drosophila melanogaster* CTP synthase (*dmCTP*) harbors a class I amidotransferase domain that connects to an acceptor amination domain.<sup>12</sup> The tunnel in *dmCTP* has some similarities with FGAM synthetase. For instance, in the absence of the substrates, it has several bottleneck residues such as V58, E57, and P52 (Figure 4B) that do not allow the tunnel to be fully formed.<sup>12</sup> Like FGAM synthetase, it also has histidine as a gating residue which exhibits a swinging door motion for opening and closing of the  $\text{NH}_3$  tunnel. When ATP and/or UTP binds in the active site of

the amination domain, it results in the conformational change leading to tunnel formation. However, a unique feature of this tunnel architecture is that the tunnel formation creates a binding site for GTP. This GTP molecule acts as a plug, and binding of GTP blocks access from the external environment and stabilizes the NH<sub>3</sub> tunnel.<sup>12</sup>

Apart from tunnels that are transient, there are also examples of preformed tunnels, with the classic example being CPS that catalyzes the conversion of bicarbonate to carbamoyl phosphate via a carbamate intermediate.<sup>6a</sup> This conversion utilizes glutamine and two molecules of ATP. CPS has one small subunit and another large subunit. The former has one active site (S1), while the latter has two active sites (L1 and L2).<sup>6a</sup> All three active sites are connected with the help of two internal tunnels. The final tunnel is 96 Å long, with one part transporting NH<sub>3</sub> and the other transporting carbamate. NH<sub>3</sub> is transferred from the S1 active site to the L1 active site in the large subunit via an NH<sub>3</sub> tunnel. A triangular gate formed by three residues, i.e., A314, A251, and C232, is present in the middle of the NH<sub>3</sub> tunnel (Figure 4C).<sup>6a</sup> A notable feature here is that while the first half of the ammonia tunnel from the S1 active site to the triangular gate is hydrophilic, the latter half, to the active site L1, is hydrophobic. Similarly, imidazole glycerol phosphate synthase (IGPS) is another GATase that exhibits a hybrid character within its NH<sub>3</sub> tunnel, where the first half of the tunnel from the glutaminase domain until the middle is hydrophilic, and the second half leading to the acceptor domain (cyclase domain) is hydrophobic (Figure 4D).<sup>24</sup> The hydrophobic part of the tunnel passes through the ( $\beta/\alpha$ )<sub>8</sub> barrel. In the middle of the ammonia tunnel, four charged residues, R239, E293, K360, and E465, act as a gate that facilitates the transition between the two halves.<sup>24</sup>

## PERSPECTIVE AND CONCLUSIONS

Here, we discussed several examples of both EG and IG tunnel architectures. In EG tunnels, since the reactant is a stable gas molecule, present in abundance in the surrounding environment, the challenge is to maintain optimal substrate concentration and to limit the amount that reaches the highly reactive centers. Several of these enzymes harbor metal clusters, such as MoFe, NiFe, etc., that catalyze difficult reactions where the transition states involve metals that need to achieve unstable oxidation states.<sup>15a,20</sup> Therefore, to prevent the inactivation of the metal center as well as to avoid side reactions, the substrate flow is tightly regulated. On the contrary, in the IG tunnel, the scenario is opposite; here, the substrate is generated within one of the active centers and is in the limiting amount as well as it could be toxic or unstable in the presented environment. Therefore, to ensure it reaches the destination reaction center, nature has devised strategies by constructing IG tunnels which, in several instances, are transient tunnels that only form upon entry of substrates and have much more controlled and complex gating architectures.

Other deciding factors that are paramount for specificity of transport via a tunnel are the nature of residues that line the passage and diameter as well as the hydrophobicity/hydrophilicity status of the tunnel interior. However, in PSII, the situation is rather unique; a common tunnel is used for transport of both H<sub>2</sub>O and O<sub>2</sub>. Here, instead of the usual hydrophobic O<sub>2</sub> tunnel, the conduit is significantly hydrophilic to allow H<sub>2</sub>O passage but is also wider such that it enables 1100-fold increased permeation of O<sub>2</sub> relative to H<sub>2</sub>O.<sup>21</sup> Overall, a variety in tunnel architectures is observed for the

same substrate, and this is evident by examples of various kinds of tunnel architecture that are adopted in the case of EG tunnels for O<sub>2</sub> transport and IG tunnels for NH<sub>3</sub> transport.

An interesting question that comes to light by studying various tunnel architectures is how do gases move to the active site or between active sites in a unidirectional way? Is there significant reflux or leakage of the gases within the tunnel, and does diffusion through peripheral regions pose a problem with the efficiency of the transport? A well-studied protein, myoglobin, does not possess any gaseous tunnel, but it has internal hydrophobic gaseous cavities.<sup>25</sup> Theoretical and time-resolved crystallographic methods have shown that the CO, which is released after the photoinduced dissociation of the CO–myoglobin complex, migrates via these internal cavities.<sup>25</sup> As the CO travels ahead in the hydrophobic cavity, it leads to the correlated fluctuations in the cavity volume, and the cavity squeezes the CO molecule from the back and pushes it ahead. Similarly, it has been shown that the fluctuations in the main EG tunnel of AlkB regulate the flow of the substrate to the active site.<sup>18</sup> A fluctuating tunnel that is akin to breathing motions also appears to be the likely mechanism of NH<sub>3</sub> transport in FGAM synthetase system. We believe that it is also possible like gaseous cavities in myoglobin and the fluctuations in the EG tunnel of AlkB, the IG tunnels in enzymes, such as *MtCODH/ACS*, and the transient ammonia tunnel in FGAM synthetase and NAD<sup>+</sup> synthetase<sup>6c</sup> possess fluctuating motion that help to push the gas in the forward direction and facilitate its translocation from one active site to the other. Instead of the gas transport being a completely passive process, we propose that the protein tunnel acts as a breathing entity that brings directionality to the delivery process. This pulsation delivery mechanism would ensure the unidirectional transfer of gaseous substrates and prevent wastage, reflux, or any other polar molecules from entering the tunnel. These aspects of correlation in tunnel architectures and dynamic fluctuations need to be experimentally established, which we believe is an important aspect in understanding tunnel driven transport of gaseous molecules.

## ASSOCIATED CONTENT

### Supporting Information

The Supporting Information is available free of charge at <https://pubs.acs.org/doi/10.1021/acsomega.1c05430>.

Reaction schemes of ethylCoM reductase (Scheme S1) and soybean lipoxygenase-I (Scheme S2, Figure S2) and the structural comparison of methyl- and ethylCoM reductase (Figure S1) (PDF)

## AUTHOR INFORMATION

### Corresponding Author

Ruchi Anand – Department of Chemistry, Indian Institute of Technology Bombay, Mumbai 400076, India; [orcid.org/0000-0002-2045-3758](https://orcid.org/0000-0002-2045-3758); Email: [ruchi@chem.iitb.ac.in](mailto:ruchi@chem.iitb.ac.in)

### Author

Sukhwinder Singh – Department of Chemistry, Indian Institute of Technology Bombay, Mumbai 400076, India; [orcid.org/0000-0002-2269-3640](https://orcid.org/0000-0002-2269-3640)

Complete contact information is available at: <https://pubs.acs.org/doi/10.1021/acsomega.1c05430>



## Notes

The authors declare no competing financial interest.

## Biographies



Sukhwinder Singh received his M.Sc. (Hons. School) in Chemistry from Guru Nanak Dev University, Amritsar. He is currently a Ph.D. student at the Indian Institute of Technology Bombay, under the guidance of Prof. Ruchi Anand. His research interests include biochemistry and structural biology. He studies dynamics and allostery in biosynthetic pathway enzymes.



Ruchi Anand is a Professor in the Department of Chemistry at the Indian Institute of Technology Bombay (IITB), India. She obtained her Ph.D. degree from the Department of Chemistry and Chemical Biology, Cornell University. She then pursued postdoctoral research at Memorial Sloan Kettering Cancer Center, New York and UPENN, Philadelphia. She is a recipient of the National Women Bio Scientist award and also has been recently awarded the DBT-Wellcome Trust Alliance Senior Fellowship. She is also a member of the National Academy of Sciences, India, and serves on the Editorial Advisory Board of *ACS Sensors* since 2016. The research interest of her group is in structural biochemistry, and her laboratory focuses on understanding the origins of antibiotic resistance as well as forging new therapies to combat it. A significant portion of her laboratory also focuses on development of biosensors for environmental water monitoring.

## ACKNOWLEDGMENTS

S.S. acknowledges Council of Scientific and Industrial Research (CSIR) for the fellowship. R.A. acknowledges Department of Biotechnology (DBT) Grant Number BT/HRD/NWBA/39/03/2018-19, Department of Science and Technology (DST) Grant Number DST/INT/SOUTH AFRICA/P-04/2014, Ministry of Science & Technology, Government of India, and IRCC IIT Bombay for funding.

## ABBREVIATIONS

EG, external gaseous; IG, internal gaseous; CPS, carbamoyl phosphate synthetase; FGAM, formylglycinamide ribonucleotide; PRPP, phosphoribosylpyrophosphate; CTP, cytidine triphosphate; ethylCoM, ethyl-Coenzyme M; methylCoM, methyl-Coenzyme M; MMOH, methane monooxygenase hydroxylase; MMOB, methane monooxygenase binding protein; H-NOX, heme-nitric oxide/oxygen binding domain; FprA, flavodiiron protein; HIF-I, hypoxia inducible factor-I; PHD2, prolyl hydroxylase domain enzyme 2; 2/2HbN, truncated hemoglobin; 2/2HbN<sub>ΔpreA</sub>, 2/2HbN having truncated n-terminal preA region; CA, carbonic anhydrase; PSII, photosystem II; cNOR, cytochrome c dependent nitric oxide reductase; CODH/ACS, carbon monoxide dehydrogenase/acetyl CoA synthase; GATase, glutamine amidotransferase; GMPS, guanosine 5'-monophosphate synthetase; IGPS, imidazole glycerol phosphate synthase

## REFERENCES

- (1) (a) Banerjee, R.; Lipscomb, J. D. Small-Molecule Tunnels in Metalloenzymes Viewed as Extensions of the Active Site. *Acc. Chem. Res.* **2021**, *54* (9), 2185–2195. (b) Massière, F.; Badet-Denisot, M. A. The Mechanism of Glutamine-Dependent Amidotransferases. *Cell. Mol. Life Sci.* **1998**, *54* (3), 205–222.
- (2) Collazo, L.; Klinman, J. P. Control of the Position of Oxygen Delivery in Soybean Lipoxygenase-1 by Amino Acid Side Chains within a Gas Migration Channel. *J. Biol. Chem.* **2016**, *291* (17), 9052–9059.
- (3) Kalms, J.; Schmidt, A.; Frielingsdorf, S.; Van Der Linden, P.; Von Stetten, D.; Lenz, O.; Carpentier, P.; Scheerer, P. Krypton Derivatization of an O<sub>2</sub>-Tolerant Membrane-Bound [NiFe] Hydrogenase Reveals a Hydrophobic Tunnel Network for Gas Transport. *Angew. Chem., Int. Ed.* **2016**, *55* (18), 5586–5590.
- (4) Lemaire, O. N.; Wagner, T. Gas Channel Rerouting in a Primordial Enzyme: Structural Insights of the Carbon-Monoxide Dehydrogenase/Acetyl-CoA Synthase Complex from the Acetogen. *Biochim. Biophys. Acta, Bioenerg.* **2021**, *1862* (1), 148330.
- (5) (a) Mahinthichaichan, P.; Gennis, R. B.; Tajkhorshid, E. Bacterial Denitrifying Nitric Oxide Reductases and Aerobic Respiratory Terminal Oxidases Use Similar Delivery Pathways for Their Molecular Substrates. *Biochim. Biophys. Acta, Bioenerg.* **2018**, *1859* (9), 712–724. (b) Tanwar, A. S.; Sindhikara, D. J.; Hirata, F.; Anand, R. Determination of the Formylglycinamide Ribonucleotide Amidotransferase Ammonia Pathway by Combining 3d-RISM Theory with Experiment. *ACS Chem. Biol.* **2015**, *10* (3), 698–704.
- (6) (a) Fan, Y.; Lund, L.; Shao, Q.; Gao, Y. Q.; Raushel, F. M. A Combined Theoretical and Experimental Study of the Ammonia Tunnel in Carbamoyl Phosphate Synthetase. *J. Am. Chem. Soc.* **2009**, *131* (29), 10211–10219. (b) Anand, R.; Hoskins, A. A.; Stubbe, J. A.; Ealick, S. E. Domain Organization of *Salmonella Typhimurium* Formylglycinamide Ribonucleotide Amidotransferase Revealed by X-Ray Crystallography. *Biochemistry* **2004**, *43* (32), 10328–10342. (c) Chuenchor, W.; Doukov, T. I.; Chang, K.-T.; Resto, M.; Yun, C.-S.; Gerrattana, B. Different Ways to Transport Ammonia in Human and *Mycobacterium Tuberculosis* NAD<sup>+</sup> Synthetases. *Nat. Commun.* **2020**, *11* (1), 16.
- (7) Ballut, L.; Violot, S.; Shivakumaraswamy, S.; Thota, L. P.; Sathya, M.; Kunala, J.; Dijkstra, B. W.; Terreux, R.; Haser, R.; Balaram, H.; Aghajari, N. Active Site Coupling in *Plasmodium Falciparum* GMP Synthetase Is Triggered by Domain Rotation. *Nat. Commun.* **2015**, *6* (1), 8930.
- (8) Sharma, N.; Ahalawat, N.; Sandhu, P.; Strauss, E.; Mondal, J.; Anand, R. Role of Allosteric Switches and Adaptor Domains in Long-Distance Cross-Talk and Transient Tunnel Formation. *Sci. Adv.* **2020**, *6* (14), 1–12.
- (9) Krahn, J. M.; Kim, J. H.; Burns, M. R.; Parry, R. J.; Zalkin, H.; Smith, J. L. Coupled Formation of an Amidotransferase Interdomain

Ammonia Channel and a Phosphoribosyltransferase Active Site. *Biochemistry* **1997**, *36* (37), 11061–11068.

(10) Pesce, A.; Bustamante, J. P.; Bidon-Chanal, A.; Boechi, L.; Estrin, D. A.; Luque, F. J.; Sebilo, A.; Guertin, M.; Bolognesi, M.; Ascenzi, P.; Nardini, M. The N-Terminal Pre-A Region of *Mycobacterium Tuberculosis* 2/2HbN Promotes NO-Dioxygenase Activity. *FEBS J.* **2016**, *283* (2), 305–322.

(11) Engilberge, S.; Wagner, T.; Carpentier, P.; Girard, E.; Shima, S. Krypton-Derivatization Highlights O<sub>2</sub>-Channeling in a Four-Electron Reducing Oxidase. *Chem. Commun.* **2020**, *56* (74), 10863–10866.

(12) Zhou, X.; Guo, C.-J.; Chang, C.-C.; Zhong, J.; Hu, H.-H.; Lu, G.-M.; Liu, J.-L. Structural Basis for Ligand Binding Modes of CTP Synthase. *Proc. Natl. Acad. Sci. U. S. A.* **2021**, *118* (30), e2026621118.

(13) Gora, A.; Brezovsky, J.; Damborsky, J. Gates of Enzymes. *Chem. Rev.* **2013**, *113* (8), 5871–5923.

(14) Hahn, C. J.; Lemaire, O. N.; Kahnt, J.; Engilberge, S.; Wegener, G.; Wagner, T. Crystal Structure of a Key Enzyme for Anaerobic Ethane Activation. *Science* **2021**, *373* (6550), 118–121.

(15) (a) Jones, J. C.; Banerjee, R.; Shi, K.; Aihara, H.; Lipscomb, J. D. Structural Studies of the *Methylosinus Trichosporium* OB3b Soluble Methane Monooxygenase Hydroxylase and Regulatory Component Complex Reveal a Transient Substrate Tunnel. *Biochemistry* **2020**, *59* (32), 2946–2961. (b) Chovancova, E.; Pavelka, A.; Benes, P.; Strnad, O.; Brezovsky, J.; Kozlikova, B.; Gora, A.; Sustr, V.; Klvana, M.; Medek, P.; Biedermannova, L.; Sochor, J.; Damborsky, J. CAVER 3.0: A Tool for the Analysis of Transport Pathways in Dynamic Protein Structures. *PLoS Comput. Biol.* **2012**, *8* (10), e1002708.

(16) Ebert, M. C. C. J. C.; Durr, S. L.; A. Houle, A.; Lamoureux, G.; Pelletier, J. N. Evolution of P450 Monooxygenases toward Formation of Transient Channels and Exclusion of Nonproductive Gases. *ACS Catal.* **2016**, *6* (11), 7426–7437.

(17) (a) Rozza, A. M.; Menyhárd, D. K.; Oláh, J. Gas Sensing by Bacterial H-NOX Proteins: An MD Study. *Molecules* **2020**, *25* (12), 2882. (b) Domene, C.; Jorgensen, C.; Schofield, C. J. Mechanism of Molecular Oxygen Diffusion in a Hypoxia-Sensing Prolyl Hydroxylase Using Multiscale Simulation. *J. Am. Chem. Soc.* **2020**, *142* (5), 2253–2263.

(18) Torabifard, H.; Cisneros, G. A. Computational Investigation of O<sub>2</sub> Diffusion through an Intra-Molecular Tunnel in AlkB; Influence of Polarization on O<sub>2</sub> Transport. *Chem. Sci.* **2017**, *8* (9), 6230–6238.

(19) Alterio, V.; Langella, E.; Buonanno, M.; Esposito, D.; Nocentini, A.; Berrino, E.; Bua, S.; Polentarutti, M.; Supuran, C. T.; Monti, S. M.; De Simone, G. Zeta-Carbonic Anhydrases Show CS<sub>2</sub> Hydrolase Activity: A New Metabolic Carbon Acquisition Pathway in Diatoms? *Comput. Struct. Biotechnol. J.* **2021**, *19*, 3427–3436.

(20) Morrison, C. N.; Hoy, J. A.; Zhang, L.; Einsle, O.; Rees, D. C. Substrate Pathways in the Nitrogenase MoFe Protein by Experimental Identification of Small Molecule Binding Sites. *Biochemistry* **2015**, *54* (11), 2052–2060.

(21) Vassiliev, S.; Zaráiskaya, T.; Bruce, D. Molecular Dynamics Simulations Reveal Highly Permeable Oxygen Exit Channels Shared with Water Uptake Channels in Photosystem II. *Biochim. Biophys. Acta, Bioenerg.* **2013**, *1827* (10), 1148–1155.

(22) Wang, P.; Bruschi, M.; De Gioia, L.; Blumberger, J. Uncovering a Dynamically Formed Substrate Access Tunnel in Carbon Monoxide Dehydrogenase/Acetyl-CoA Synthase. *J. Am. Chem. Soc.* **2013**, *135* (25), 9493–9502.

(23) Raushel, F. M.; Thoden, J. B.; Holden, H. M. Enzymes with Molecular Tunnels. *Acc. Chem. Res.* **2003**, *36* (7), 539–548.

(24) Chaudhuri, B. N.; Lange, S. C.; Myers, R. S.; Chittur, S. V.; Davisson, V. J.; Smith, J. L. Crystal Structure of Imidazole Glycerol Phosphate Synthase: A Tunnel through a ( $\beta/\alpha$ )<sub>8</sub> Barrel Joins Two Active Sites. *Structure* **2001**, *9* (10), 987–997.

(25) Tomita, A.; Sato, T.; Ichianagi, K.; Nozawa, S.; Ichikawa, H.; Chollet, M.; Kawai, F.; Park, S.-Y.; Tsuduki, T.; Yamato, T.; Koshihara, S.-y.; Adachi, S.-i. Visualizing Breathing Motion of Internal Cavities in Concert with Ligand Migration in Myoglobin. *Proc. Natl. Acad. Sci. U. S. A.* **2009**, *106* (8), 2612–2616.